Polymerization Thermodynamics and Structural Stabilities of Skeletal Muscle Actins from Vertebrates Adapted to Different Temperatures and Hydrostatic Pressures†

Robert R. Swezey* and George N. Somero*

ABSTRACT: Skeletal muscle actins from 14 vertebrate species having average body temperatures of from −1.9 to 39 °C were purified, and the free energy, enthalpy, and entropy changes accompanying the assembly of filamentous (F) actin from monomeric (G) actin were measured. The thermal stabilities of the actins also were studied. The enthalpy and entropy of polymerization increased with average body temperature (except for actins of deep-sea fishes) and exhibited a regular enthalpy–entropy compensation relationship ($d\Delta H/d\Delta S$ = 275 K). The ΔH of the G to F transformation varied by more than 1 order of magnitude among species, ranging from 14.57 kcal/mol for actin of the thermophilic desert lizard *Dipsosaurus dorsalis* to 0.67 kcal/mol for the deep-sea fish *Coryphaenoides armatus*. However, the critical monomer concentration for polymerization (C_c), which is established by the ΔG of polymerization, was strongly conserved, at normal body temperatures, among all species. Heat stabilities increased with rising average body temperature (the deep-sea fishes' actins were again exceptional and were extremely heat resistant). These findings suggest that the conservation of an ability to polymerize effectively under different temperature and pressure conditions is achieved by two mechanisms affecting polymerization energetics: alterations in the types of bonds, e.g., changes in the relative importance of hydrophobic interactions vs. charged or polar interactions that occur at the subunit contact sites, and changes in the energy costs of altering the actin monomer conformation during the assembly process. A reduced dependence on hydrophobic interactions at subunit contact sites may be important in fishes living at low temperatures and, especially, in deep-sea fishes, which encounter both low temperatures and high hydrostatic pressures.

Coordinated cellular events are dependent on a suite of macromolecular self-assembly processes, including the assemblies of multimeric enzymes, cellular membranes, and contractile elements such as muscle thin filaments and microfilaments. In these assembly processes there exists the requirement for the components to recognize each other and to interact in a thermodynamically favorable manner.

Actin assembly was one of the first protein assembly processes to be studied thermodynamically. Investigations by Oosawa and colleagues (Kasai et al., 1962; Kasai, 1969; Oosawa & Kasai, 1971) showed that the polymerization of actin subunits (G-actin) to form filamentous (F) actin was an entropy-driven process. The large increase in entropy during the G to F transformation more than offsets the positive enthalpy change that accompanies the reaction. Actin assembly thermodynamics appear typical in this regard, for the assemblies of many other multisubunit protein systems, e.g., tobacco mosaic virus (Lauffer, 1975), tubulin (Weisenberg, 1972; Engelborghs et al., 1976), and myosin (Josephs & Harrington, 1968), also are entropy driven. In these assembly processes the major contributor to the stabilization free energy of the polymeric structures is thought to be hydrophobic interactions. Thus, the domains of intersubunit contact for those oligomeric proteins whose tertiary structures are known contain a high density of hydrophobic residues (Chothia & Janin, 1975). When these subunit contact sites are brought into juxtaposition, the exclusion of organized water from around the hydrophobic groups results in a large entropy increase, which provides the driving force for assembly; polar and/or charged group interactions establish the specificity of protein–protein binding. In addition to the energy changes resulting from alterations in water structure, protein assembly thermodynamics may also receive contributions from energy changes that accompany alterations in subunit conformation if variations in tertiary structure are a concomitant of the assembly process (Fisher et al., 1981).

In view of these two types of contributions to the overall energetics of protein assembly processes, it is appropriate to ask whether a given type of assembly process, e.g., the G to F transformation, is invariant among species adapted to different environmental conditions (temperature, hydrostatic pressure, and cytosol osmotic composition and concentration). A number of studies have shown that the assembly of F-actin and other multisubunit systems (Oosawa & Kasai, 1971; Lauffer, 1975) is extremely sensitive to these environmental variables. These sensitivities can be attributed, in part, to the effects of temperature, pressure, and solutes on hydrophobic interactions and, in part, to the effects of these variables on the stability of protein tertiary structure. While these effects have been noted principally in mammalian systems, which have been studied almost exclusively, the sensitivities of assembly processes to these physical and chemical perturbants are of sufficient magnitude to suggest that evolutionary change in assembly processes may be necessary to permit the maintenance of comparable assembly equilibria in species from widely different environments.

To explore this facet of molecular evolution and to gain further insight into the fundamental features of F-actin assembly, we purified skeletal muscle actin from 14 vertebrate species whose body temperatures range from −1.9 (Antarctic fishes) to approximately 47 °C (desert iguana) and whose environmental pressures range from 1 (terrestrial species) to over 500 atm (deep-sea fishes). We determined the free energy, enthalpy, and entropy changes that occur during the G to F transformation, and we estimated the thermal stability of monomer structure. We report consistent and apparently adaptive differences in assembly energetics and monomer stability. The enthalpy and entropy changes accompanying

† From the Marine Biology Research Division, Scripps Institution of Oceanography, University of California, San Diego, La Jolla, California 92093. *Received February 2, 1982.* This research was supported by National Science Foundation Grants PCM 80-01949 and PCM 80-23166.

0006-2960/82/0421-4496$01.25/0

the G to F transformation rise with increasing body temperature among the species studied. Heat stability of G-actin also rises with increasing body temperature among species, yet stability is also high for actins of the deepest living fishes. We conclude that evolutionary changes have occurred at subunit contact sites, where energy changes due to water displacement are important, and in overall G-actin structural rigidity, which affects the energy changes due to conformational change during polymerization. The net effect of these adaptations is a strong conservation of the critical monomer concentration (C_c) for polymerization in all species at their physiological temperatures.

Materials and Methods

Experimental Analysis. Fourteen vertebrate species having a wide range of average body temperatures and experiencing pressures ranging from 1 to approximately 500 atm were chosen for this study. All specimens were killed and frozen shortly after capture. Specimens were held at −80 °C until used for actin purification.

The animals used (their body temperatures and, where relevant, depths of occurrence) were as follows: rabbit (37 °C); chicken (39 °C); desert iguana, *Dipsosaurus dorsalis* (30–47 °C); elasmobranch fish, *Rhinobatos productus* (10–20 °C); teleost fishes, *Sebastolobus alascanus* (3–10 °C), *Sebastolobus altivelis* (3–10 °C), *Caranx hippos* (25–28 °C), *Cyprinodon macularius* (10–40 °C), *Thunnus alalunga* (15–25 °C), *Gymnodraco acuticeps* (−1.9 °C), *Pagothenia borchgrevinki* (−1.9 °C), *Coryphaenoides acrolepis* (2–3 °C, 250–2100 m), *Coryphaenoides armatus* (2–3 °C, 1900–4800 m), and *Halosauropsis macrochir* (2–3 °C, 1600–5300 m). Temperature data for *D. dorsalis* are from Norris (1953); data for other temperature and depth regimes can be found in Somero (1982).

Actin Purification. Muscle samples were dissected from the frozen specimens, and acetone powders ("low-salt EDTA" preparation of Strzelecka-Golaszewska et al., 1980) were prepared as sources of actin. Actin was purified by the method of Spudich & Watt (1971) to greater than 95% homogeneity (by the criterion of $NaDodSO_4$[1]–polyacrylamide gel electrophoresis). Skeletal-type muscle was used in all cases.

DNase I Assay of Native G-Actin Concentration. G-Actin concentrations were measured with a modified version of the DNase I inhibition assay of Blikstad et al. (1978). Only native (=polymerization competent) G-actin can inhibit DNase I (Hitchcock et al., 1976; Lazarides & Lindberg, 1974). Stock solutions of DNase I contained 0.04 mg/mL of the enzyme dissolved in 50 mM Tris-HCl buffer (pH 7.5 at 25 °C) containing 0.5 mM $CaCl_2$ and 0.01 mM PMSF (to inactivate a protease contaminant of the commercial DNase I preparation). one-milliliter aliquots of the stock DNase I solution were quick frozen in liquid nitrogen and stored at −20 °C. These stock solutions were stable for at least several weeks. Substrate DNA stock contained 0.08 mg/mL DNA in 5 mM Tris-HCl buffer (pH 7.5 at 25 °C) containing 0.33 mM $MnCl_2$. The stock solution was stored at 4 °C.

In the standard DNase I assay, 25 μL of the enzyme was introduced via a Hamilton microsyringe to the corner of a 4-mL quartz cuvette, which was held at 25 °C in a thermostated cell holder of the spectrophotometer. The quantity of actin (or buffer blank) being measured (usually in a volume of 10 μL) was then syringed directly into the DNase I droplet. One second later, 3 mL of the DNA substrate solution, preequilibrated at 25 °C, was added to the cuvette. The cuvette was removed quickly from the holder and inverted twice to mix the contents, and the rate of change in OD_{260} was then recorded at 25 °C. Full DNase I activity was defined as the decrease in OD_{260} per minute when an equal volume of buffer, lacking only the actin, was added to the assay system. This rate was used as the reference for calculating the percent inhibition of the enzyme by actin.

The critical monomer concentrations (C_c) for polymerization were calculated by determining the G-actin content as a function of total actin concentration; extrapolating the measurements of G actin to the line [G-actin] = [total actin] will correct for the low levels of inhibition by F-actin (see Figure 2). In these experiments, "total actin" refers to the concentration of native, polymerization competent actin present in the solution [prepared in buffer G (5 mM imidazole hydrochloride, pH at 7.0 at 20 °C, 0.2 mM $MgCl_2$, 0.1 mM ATP, 0.2 mM DTT, and 10 mg/L NaN_3)] prior to addition of 0.1 M KCl, which induced polymerization.

Spectrophotometric Assay of Actin Polymerization. Actin assembly also was monitored by recording the increase in OD_{232} accompanying polymerization (Higashi & Oosawa, 1965; Spudich & Cooke, 1975). Polymerization was initiated by addition of KCl, to a final concentration of 0.1 M, to a KCl-free solution of G-actin, and the absorbance was monitored in a Beckman Acta M-VI spectrophotometer. The spectrophotometric technique for monitoring the G to F transformation was a convenient method for ascertaining the time required to reach equilibrium at different temperatures. The incubation times used in the polymerization studies were well in excess of the minimal time to attain equilibrium at all temperatures. The incubation times at the different experimental temperatures were as follows: 25 °C, 2 h; 20 °C, 2 h; 15 °C, 4 h; 10 °C, 8 h; 5 °C, 14 h.

Heat-Stability Studies. The heat stabilities of the G-actins were determined by assaying the residual DNase I inhibition of the samples as a function of time of incubation at 38 °C in buffer G. The total actin concentration, determined spectrophotometrically (see below), was 0.2 mg/mL for all samples.

Isoelectric Focusing. Isoelectric focusing was conducted by the method of Wrigley (1971) in 5% polyacrylamide gels containing 1% ampholines (pH 4–6 gradient; Bio-Rad Laboratories). The cathode buffer was 0.4% ethanolamine; the anode buffer was 0.2% H_3PO_4. Gels were prefocused at 90 mV until the current fell close to zero (about 30 min). The samples (containing 10% glycerol to increase density) then were applied to the basic end of the gels and were focused at 90 mV for 6 h. Ampholines were removed by soaking the gels overnight in 20% Cl_3CCOOH. The gels then were stained for protein with Coomassie Blue G-250, as described by Reisner et al. (1975). The pH gradient was determined by slicing a focused gel to which no protein had been added into 20 sections, extracting each section in 1 mL of distilled water, and measuring the pH of the extract.

Protein Concentration Measurements. We determined protein concentrations spectrophotometrically by using $\epsilon_{280}^{0.1\%} = 0.63$ for rabbit and chicken actin (Houk & Ue, 1974) or by using the relationship $(OD_{235} - OD_{280})/2.20$ = [actin] in milligrams per milliliter (Whitaker & Granum, 1980) for actins from the other species; the value of 2.20 in the denominator was determined empirically for rabbit actin. The latter method was chosen as it has been shown to measure peptide

[1] Abbreviations: DTT, dithiothreitol; Hepes, *N*-(2-hydroxyethyl)-piperazine-*N*′-2-ethanesulfonic acid; $NaDodSO_4$, sodium dodecyl sulfate; PMSF, phenylmethanesulfonyl fluoride; Tris, tris(hydroxymethyl)-aminomethane; EDTA, ethylenediaminetetraacetic acid.

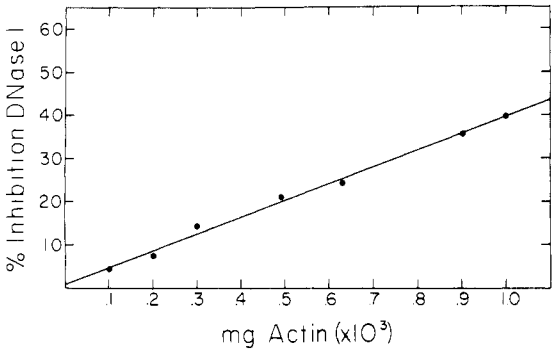

FIGURE 1: Standard curve for the DNase I inhibition assay for G-actin. The indicated amounts of freshly prepared rabbit skeletal muscle G-actin, contained in 10 μL of G buffer, were added to 25 μL of DNase I stock 1 s prior to the addition of 3 mL of DNA substrate, and the percent decrease in the DNase I reaction rate was determined.

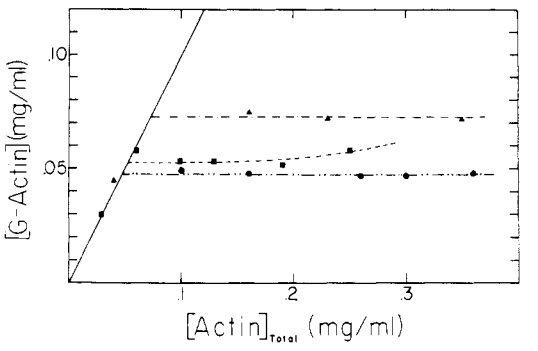

FIGURE 2: Measurement of the critical actin monomer concentration by DNase I inhibition. Muscle actin samples from rabbit (●), *S. alascanus* (■), or *C. armatus* (▲) were brought to the final total actin concentrations indicated on the abscissa. Polymerization was effected by addition of KCl to a final concentration of 0.1 M, and the content of G-actin remaining in the solutions was determined by percent inhibition of the DNase I reaction. The solid line represents the amount of G-actin in unpolymerized samples (i.e., a line of unity). Critical monomer concentrations are determined by extrapolation of G-actin measurements back to this line. The measured C_c values were 0.048 mg/mL for rabbit, 0.053 mg/mL for *S. alascanus*, and 0.072 mg/mL for *C.* armatus. Data were obtained at 10 °C.

bond constant and, therefore, should be less variable between species than other assays such as the Lowry or dye-binding method. On the assumption that there are no major differences in the conformation of the peptide backbones among the 15 actins examined here, rabbit muscle actin is the protein of choice to calibrate this protein assay since its concentration can be established unambiguously by using its known extinction coefficient.

$NaDodSO_4$–Polyacrylamide Gel Electrophoresis. $NaDodSO_4$–polyacrylamide gel electrophoresis on 12% acrylamide gels was performed according to the method of Weber & Osborn (1969). Gels were stained with either Fast Green FCF or Coomassie Blue R-250.

Results

DNase I Assay. The standard DNase I assay for G-actin content of Blikstad et al. (1978) was modified to increase the precision of critical monomer concentration measurements. Substitution of 0.33 mM $MnCl_2$ for 4 mM $MgSO_4$ plus 1.8 mM $CaCl_2$ as the divalent cation activator of the enzyme converts the nuclease's kinetics from sigmoidal to linear (Junowicz & Spencer, 1973). The establishment of a linear rate of nuclease activity from the beginning of the assay has two major benefits. First, with the Blikstad et al. method, the length of time during which the change in absorbance remains linear is brief due to the sigmoidal reaction kinetics, and this nonlinearity tends to reduce the reproducibility of maximal rate determinations. Second, since there is not initial lag phase in our modified assay system, the reaction rate (and, therefore, the precent inhibition of the nuclease) can be measured immediately, rather than after at least 75 s into the reaction time, as under the Blikstad et al. method. While inhibition by G-actin is essentially instantaneous, F-actin also can inhibit the nuclease, albeit F-actin inhibition occurs much more slowly (Hitchcock et al., 1976; Blikstad et al., 1978). The F-actin–DNase I interaction rate, as determined viscometrically, is greatest during the first few minutes after mixing the reactants together (Mannherz et al., 1975). Therefore it is important when measuring critical monomer concentrations to assess the percent inhibition of DNase I as quickly as possible to minimize inhibition by F-actin. In the Blikstad et al. procedure the lag phase of the reaction becomes extended as the percent inhibition by actin increases (Lindberg, 1964); hence, the accuracy of the C_c determinations is greatly improved with our linear kinetics assay system.

A standard curve for percent inhibition of DNase I with increasing amounts of G-actin is shown in Figure 1. The specific inhibitions (percent inhibition per microgram of protein) of the different freshly prepared actins were always within 10% of the value found for rabbit muscle actin, indicating that the stoichiometry of actin–DNase I binding found for rabbit actin (1:1) (Mannherz et al., 1975) is probably characteristic of other muscle actins as well. The slight variability in specific inhibition may arise from differences among species in the structural stability of the monomers (see below).

For demonstration of the validity of our approach for determinations of the C_c, Figure 2 shows the measurement of G-actin content as a function of total actin concentration in muscle actin samples polymerized at 10 °C from rabbit and two fishes. The measured G-actin contents do not change once the C_c is reached, despite a nearly 10-fold increase in actin concentration above the C_c. Our determination of the C_c of rabbit muscle actin at 25 °C, 0.022 mg/mL, agrees well with value reported by other workers who used different techniques, 0.020 mg/mL (Gordon et al., 1976; Uyemura et al., 1978).

It should be noted that interference by F-actin was more conspicuous at higher assay temperatures (unpublished observations). Thus, we advise measuring G-actin content at several total actin concentrations to minimize artifacts.

Thermodynamics of G to F Transformation. According to the nucleated condensation model of actin polymerization (Oosawa & Kasai, 1971), the equilibrium constant of the G to F transformation (K_p) equals the reciprocal of the critical monomer concentration; i.e., $K_p = 1/C_c$. In fact, actin polymerization in these studies is not an equilibrium process in the strictest sense of the term, since ATP-G-actin is the monomer species that is added to the polymer while ADP-G-actin is the monomer species released from the polymer. However, studies using a nonhydrolyzable ATP analogue bound to actin monomers showed that the dephosphorylation reaction is not thermodynamically coupled to the polymerization reaction (Cooke, 1975). Therefore, the equilibrium constant for assembly will not be perturbed by the disparity in the nucleotides bound in the "on" vs. the "off" reactions occurring at the quasi-equilibrium steady state. Accordingly, the application of equilibrium thermodynamics to this process should remain a valid means of dissecting the energetics of actin polymerization. Thus, by determining the K_p at different temperatures, one can compute the enthalpy and entropy changes during polymerization from estimates of the slopes and intercepts,

Table I: Polymerization Thermodynamics, Heat Stabilities, and Isoelectric Points of Skeletal Muscle Actins of 14 Vertebrate Species

species (no.)[a]	ΔH[b]	ΔS[c]	C_c[d] (T_B)	heat stability k_1[e]	heat stability k_2[e]	pI value
rabbit (1)	9.29	60.00	0.011 (37)	1.76	0.62	5.15
chicken (2)	9.09	59.28	0.012 (39)	1.60	0.63	5.14
Dipsosaurus dorsalis (3)	14.57	80.18	0.003 (35)	0.00		5.16
Sebastolobus alascanus (4)	2.91	37.12	0.062 (5)	4.78	3.20	5.15
Sebastolbus altivelis (5)	3.16	38.19	0.056 (5)	4.70	3.25	5.16
Caranx hippos (6)	3.56	39.10	0.048 (25)	3.82	0.98	5.17
Cyprinodon macularius (7)	2.70	35.96	0.045 (37)	4.45	1.70	nd[f]
Rhinobatos productus (8)	5.41	46.96	0.020 (15)	4.07	0.83	5.10
Thunnus alalunga (9) (white muscle)	3.09	37.85	0.041 (24)	5.74	3.88	5.14
Thunnus alalunga (10) (red muscle)	3.02	36.86	0.059 (24)	4.68	3.95	5.13
Gymnodraco acuticeps (11)	2.01	33.90	0.066 (−2)	4.66	2.86	5.16
Pagothenia borchgrevinki (12)	1.75	32.97	0.066 (−2)	9.20	4.74	nd
Coryphaenoides armatus (13)	0.67	28.89	0.070 (2)	0.58		5.16
Coryphaenoides acrolepis (14)	3.22	39.26	0.038 (2)	0.22		5.13
Halosauropsis macrochir (15)	1.10	32.63	0.022 (2)	0.28		5.15

[a] Species numbering is used in Figures 3, 5, 6, and 9. [b] Kilocalories per mole. [c] Entropy units. [d] Critical monomer concentration in milligrams per milliliter at average body temperature (T_B) in degree Celsius. [e] Rate constants × 10^3 per minute. [f] nd, not determined.

respectively, of a plot of ln K_p vs. reciprocal temperature (1/K) (van't Hoff relationship).

Table I contains the ΔH and ΔS values for the 15 actin assembly reactions based on K_p values determined at 5 °C intervals between 5 and 25 °C. Also given are the calculated C_c values at each organism's average body temperature. Enthalpy changes for the G to F transformation vary by over 1 order of magnitude between the deep-sea fishes (0.67 kcal/mol), on the one hand, and terrestrial vertebrates (9–15 kcal/mol), on the other. In general, the ΔH of polymerization exhibits a regular increase with rising average body temperature among the species, although the deep-sea fishes (body temperatures near 2–3 °C) have lower ΔH characteristics than those of the lowest body temperature species, the Antarctic fishes (−1.9 °C).

A strong covariation in the magnitudes of ΔH and ΔS was found (Table I); high values of ΔH were invariably associated with high values for ΔS. This trend is shown more clearly in Figure 3, which plots ΔH vs. ΔS. This type of plot, known as an enthalpy–entropy compensation plot (Lumry & Biltonin, 1969), has a slope measured in kelvin. This slope, termed the "compensation temperature" (Lumry & Biltonin, 1969), may provide insights into the types of reactions that contribute to ΔH and ΔS, as discussed below. Whereas the compensation phenomenon at times may be a statistical artifact of experimental error if the compensation temperature is close to the harmonic mean of the assay temperatures (Krug et al., 1976), the compensation effect noted in our study is likely to be real since the compensation temperature of 275 K (2 °C) is far removed from the harmonic mean of the assay temperatures (15 °C).

The data presented in Table I and Figure 3 suggest that the species examined can be grouped into several distinct classes: very deep living fishes (13 and 15), Antarctic fishes (11 and 12), temperate zone fishes (4–7, 9, 10, and 14), elasmobranch fishes (8), birds and mammals (1 and 2), and thermophilic desert reptiles (3). We discuss the bases for this intergroup variation below.

Despite the wide variations in ΔH and ΔS with body temperature, all actins displayed a C_c value below 0.1 mg/mL at the organisms' physiological temperatures (Table I). This interspecific conservation of C_c in fact is a reflection of the differences in ΔH and ΔS of polymerization. Thus, for low body temperature species like the Antarctic fishes, the low ΔH of polymerization ensures that the G to F transformation can occur effectively even at subzero temperatures. At −1.9 °C,

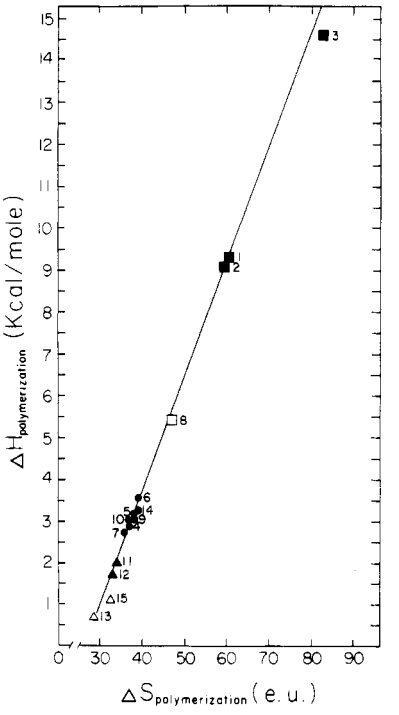

FIGURE 3: Enthalpy–entropy compensation plot comparing assembly thermodynamics of actins from 15 species of vertebrates. ΔH and ΔS of polymerization were calculated by applying the van't Hoff relationship (see the text) to critical monomer concentration measurements made at five temperatures. The numbers in the figure refer to the species listed in Table I. Different symbols are used to group the organisms as follows: terrestrial vertebrates (■), elasmobranch fish (□), temperate water fishes (●), Antarctic fishes (▲), and very deep living fishes (△).

the normal body temperature of these Antarctic fishes, the C_c value for actin assembly is 0.066 mg/mL; for rabbit muscle actin at this temperature, C_c is 0.094 mg/mL.

It is not clear if the C_c values for the actin polymerization reactions of the deep-sea fishes are physiologically meaningful since these values were determined at 1 atm pressure, whereas the fishes experience pressures of up to several hundred atmospheres.

Heat Stability of G-Actins. The heat stability of G-actin was determined by estimating the residual DNase I inhibiting ability of actin solutions that were incubated at 38 °C for different periods of time. Figure 4 shows that the decrease in DNase I inhibiting (=native) actin parallels the decrease

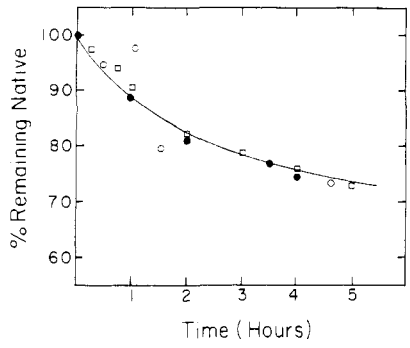

FIGURE 4: Time course of denaturation of G-actin from rabbit (●, ○) and chicken (□) skeletal muscle. Purified G-actin (0.2 mg/mL in buffer G) was incubated at 38 °C, and at the times indicates, aliquots were removed and assayed for native actin content either by measuring the amount of actin that would polymerize upon addition of KCl to 0.1 M (closed symbols) or by the ability to inhibit DNase I (open symbols).

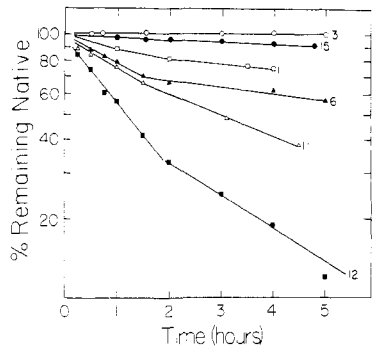

FIGURE 5: Comparison of G-actin denaturation kinetics of six representative species. Samples were treated as described in Figure 4, and the data were plotted semilogarithmically to allow computation of the first-order rate constants (listed in Table I) from the slopes of the plots. The numbers in the figure refer to the species listed in Table I.

in polymerization-competent actin. Data for rabbit and chicken actin, which have identical amino acid sequences (Vandekerckhove & Weber, 1979), are given. Aliquots taken at various times and placed in an ice bath failed to show an increase in DNase I inhibition (data not shown); thus the loss in DNase I inhibition is due to irreversible denaturation and not to a heat-induced polymerization of G-actin.

The heat-stability profiles of actins from several species are shown in Figure 5, in which the data are plotted semilogarithmically to allow computation of the first-order rate constants of denaturation. These rate constants are presented in Table I. Two important aspects of actin thermal stability are noted in Figure 5. First, there is great interspecific variability in the resistance of G-actin to heat denaturation. At one extreme, actin from desert iguana, *D. dorsalis*, exhibited no loss of DNase I inhibiting ability after 5 h at 38 °C. At the other extreme, G-actin from the Antarctic fish, *Pagothenia borchgrevinki*, lost 85% of its DNase I inhibiting ability under these conditions. The data in Figure 5 and Table I show that actins from the other species have structural stabilities lying between these two extremes and that these stabilities are roughly in proportion to the average body temperatures of the organisms. However, the two deepest living fishes, *Coryphaenoides armatus* and *H. macrochir*, depart from this trend between actin stability and body temperature; actins from these two species have much higher heat stabilities than actins of other teleost fishes.

A second feature of the heat denaturation data for many of the species is a distinct biphasic kinetics of loss of DNase

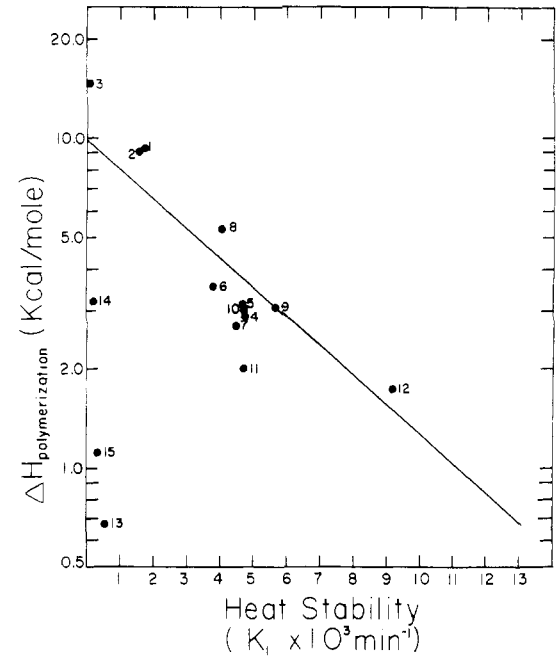

FIGURE 6: Correlation between thermal stability of G-actin and enthalpy of polymerization. Data are from Table I, and the numbers refer to the species listed in Table I. The solid line is a linear regression of the data from species 1–12; the r^2 value is 0.78.

I inhibiting ability. For actins of such species there appear to be two first-order processes occurring during the loss of DNase I inhibiting ability. These biphasic kinetics were not found for the four actins having the highest thermal stabilities.

We observed that, in general, the actins with lower thermal stabilities were those with low enthalpies of polymerization. This relationship is shown in Figure 6, which plots ln ΔH vs. K_1 (heat stability). A distinct trend (r^2 = 0.78) is seen for all species except the deepest living fishes. The latter data were not included in the regression analysis.

Isoelectric Focusing. All of the actins, when freshly prepared, had molecular weights of approximately 42 000, as judged by NaDodSO$_4$–polyacrylamide gel electrophoresis (data not shown). On isoelectric focusing gels, all of the actins focused as a single major band near a pH (=p*I*) of 5.15 (range = pH 5.10–5.17; Table I). A second band with a more alkaline p*I* (between p*I* 5.35 and 5.69) appeared as a function of storage time of the actin samples, a result suggestive of slow proteolysis of the actin with time (Carlsson et al., 1977). This minor second band seen on isoelectric focusing gels was found to have a molecular weight of approximately 36 500, by the criterion of NaDodSO$_4$ gel electrophoresis. The elasmobranch fish actin was especially susceptible to this apparent proteolysis.

Discussion

Recent studies of actin amino acid sequences have shown a high degree of sequence conservation for this protein across a broad evolutionary spectrum. For example, only a small number of amino acid substitutions exist between actins of the protozoan *Physarum polycephalum* and mammalian cytoplasmic actin (3.2% of total sequences are divergent) (Vanderkerckhove & Weber, 1978), and rabbit and chicken muscle actins have identical sequences (Vanderkerckhove & Weber, 1979). In view of the number of specific binding sites on the actin monomer, including muscle actin sites for interaction with myosin, tropomyosin, troponin I, DNase I, ATP, and divalent cations, plus four self-assembly sites, the requirements for structural conservation are evident. Nonetheless, our findings demonstrate wide interspecific structural and functional dif-

ferences among skeletal muscle actins that appear to be adaptive. In particular, the differences in polymerization energetics effect the conservation of a key property of actin, the maintenance of a low value for the critical monomer concentration, and, therefore, of the ability to polymerize effectively under physiological conditions of temperature and pressure.

One of the most striking trends noted in this study is the regular covariation in the enthalpy and entropy changes accompanying the G to F transformation among the different species. With the exception of the deepest living fishes studied, ΔH and ΔS exhibit a regular increase with increasing average body temperature (Figure 3; Table I). This interspecific variation merits discussion for, although thermodynamic data cannot be used to prove a mechanism, the enthalpy and entropy changes found in this study do offer some insights into the roles played by the two sources of free-energy change during the G to F transformation, namely, bonding at the monomer contact sites and changes in monomer conformation, to the polymerization thermodynamics of the different species' actin assembly reactions.

For all of the actins examined, the enthalpy change during polymerization was positive. The driving force for polymerization, therefore, is an entropy increase sufficient to yield an overall decrease in the free energy of the system during polymerization. The wide interspecific variation in the enthalpies and entropies of polymerization is consistent with varying degrees of dependence on hydrophobic interactions and on charged or polar interactions among species. Since interactions between charged or polar groups are exothermic, entropy-driven processes are thought to involve primarily hydrophobic interactions (Lauffer, 1975). The changes in water structure accompanying the formation of hydrophobic interactions are endothermic, but the concomitant change in entropy is highly positive (Frank & Evans, 1945; Kauzmann, 1959). For processes that involve the formation or rupture of hydrophobic interactions, a regular covariation between ΔH and ΔS is noted (Lumry & Rajender, 1970), and a plot such as that shown in Figure 3 typically yields a compensation temperature near 275 K (Lumry & Rajender, 1970; Lauffer, 1975). Indeed, the mechanism commonly advanced to explain the entropy-driven character of hydrophobic interactions involves the reorganization of water molecules surrounding the nonpolar residues such as to maximize the extent of water–water hydrogen bonding, while severely limiting the number of configurations available to these water molecules relative to those available in the bulk phase. Upon association of two nonpolar moieties, the intermediary water molecules become expelled and released into the bulk solvent phase. This event requires the breaking of hydrogen bonds but greatly increases the released water molecules' degree of orientational freedom. Thus, due to these water structure changes, both ΔH and ΔS of hydrophobic interaction formation are positive.

We suggest that the covariation in ΔH and ΔS noted for actin polymerization reactions of the different species is, at least in part, a reflection of different dependencies on hydrophobic interactions for stabilizing F-actin. Species having the lowest body temperatures (deep-sea and Antarctic fishes) have actin polymerization reactions with the lowest ΔH and ΔS. These low values for ΔH and ΔS are consistent with a reduced dependence on hydrophobic bonds, at least relative to the dependence on charged group or polar group interaction, at the subunit contact sites. Since interactions between charged and/or polar groups are exothermic, while hydrophobic interactions are endothermic, it would appear adaptive for low body temperature species to depend on the former type of bonding to a greater extent for maintaining the integrities of multiprotein complexes. For instance, if the strongly endothermic reaction involved in the polymerization of mammalian or avian muscle actin were to characterize the actin assemblies of low body temperature animals, the C_c values would be significantly higher than those found for the low temperature species' actins at physiological temperatures (Table I). Additionally, a strong reliance on hydrophobic interactions in deep-sea animals could prove to be especially problematical. The increase in entropy that occurs during the formation of hydrophobic interactions due to changes in water structure is accompanied by an increase in system volume (Stevens & Lauffer, 1965; Lauffer, 1975). Because the magnitude of the volume change (ΔV) that occurs during polymerization establishes the pressure sensitivity of the assembly process, a reduction in ΔV of assembly would appear to be advantageous to deep-living species. In at least certain protein processes, large enthalpy and entropy changes are associated with large volume changes (Greaney & Somero, 1979). Thus, the large ΔH and ΔS of assembly noted, e.g., with the mammalian actin assembly process, suggest that the volume change of assembly also may be large. This conjecture is supported by studies of pressure effects on rabbit muscle actin, where a ΔV of assembly of approximately 86–200 cm^3/mol was found (Ikkai & Ooi, 1966; Ikkai et al., 1966). This large ΔV of assembly would lead to an increase in the C_c of between 2 and 3 orders of magnitude under typical habitat conditions of the deepest living fishes we studied (500 atm pressure; 2 °C). We are currently investigating the interspecific differences in ΔV of assembly to determine whether the small ΔH and ΔS of assembly noted for actins of the deepest living species are associated with low ΔV values.

Whereas the above arguments based on thermodynamic considerations and adaptive mechanisms for coping with variations in temperature and hydrostatic pressure are consistent with the polymerization energy changes we observed in these studies, it is also essential to consider the second type of contributor to polymerization energy changes, namely, the alterations in G-actin conformation during polymerization. There is convincing evidence that actin polymerization entails a conformational change in the monomer (Higashi & Oosawa, 1965; Rich & Estes, 1976; Harwell et al., 1980; Brenner & Korn, 1981). Thus, a more complete description of the G to F transformation is

$$\text{G-actin} \xrightarrow{K_1} \text{G*-actin} \xrightarrow{K_2} \text{F-actin}$$

where G*-actin is the actin monomer in the altered conformation required for polymerization. The overall ΔH of polymerization thus will be ΔH_1 (the enthalpy change required to convert G-actin to G*-actin) plus ΔH_2 (the enthalpy change of actin–actin association). When viewed in this more complete framework, the observed interspecific variation in ΔH of polymerization could result, at least in part, from differences in ΔH_1, as well as differences in ΔH_2. Although at present there is no way to quantify the contributions of ΔH_1 and ΔH_2 to the overall enthalpy change of polymerization, or to estimate the relative roles of these two contributors to ΔH of assembly in the different species' actin assembly reactions, the differences found in G-actin thermal stability do suggest that interspecific differences in ΔH_1 may contribute to the variations in assembly energetics.

We reasoned that, as a first approximation, the energy cost of converting G-actin to G*-actin is related to the inherent strength of monomer structure, as here measured by heat

stability. Comparisons of heat stability showed that, with the exception of the deepest living fishes, resistance to thermal denaturation increased with rising average body temperature (Table I). The actins of the two deepest living fishes exhibited extremely high heat stability, despite the low body temperatures of the animals. We interpret this high degree of structural stability as an adaptation to elevated pressure, since protein structures are destabilized by high pressures, particularly at low temperatures (Brandts, 1969).

When the overall ΔH of assembly is compared to the heat stabilities of the monomers (using k_1 of denaturation as the measure of monomer heat stability) as in Figure 6, a strong correlation is found. Actins with less rigid structures, and, thereby, presumably having smaller energy requirements for the G to G* conversion, polymerize with a smaller ΔH. We propose that this correlation between heat stability, on the one hand, and ΔH of polymerization, on the other, is a reflection of a causal relationship.

One surprising feature of the heat denaturation studies is the biphasic nature of loss in DNase I inhibition with time noted for most of the actins (Figure 5). One possible explanation for this effect is that there are two sequential unfolding steps, the first of which leads to an actin conformation less able to inhibit DNase I while the second unfolding step renders the actin completely unable to inhibit DNase I. However, since the time course for loss of polymerization competence parallels the loss of DNase I inhibiting ability (Figure 4), we postulate that the two-step unfolding process first results in an actin "less able" to polymerize before becoming totally polymerization incompetent. Presumably, monomers less able to polymerize could form polymers, but the intersubunit bonds would be weaker, leading to a higher value for the C_c. Physical studies of actin conformations have not provided any evidence for an intermediate state between native G-actin and partially unfolded, but irreversibly nonpolymerizable, actin (Lehrer & Kerwar, 1972), but physical methods may be less able to detect subtle conformational changes than are enzyme methods like the DNase I assay.

Despite variation in assembly thermodynamic parameters and heat stability, all of the actins examined were found to have essentially identical isoelectric points (p*I* values) (Table I). The differences in thermodynamic and structural characteristics do not appear to be due to shifts in the ratios of positively to negatively charged amino acid residues.

The elasmobranch fish studied, *R. productus*, had actin polymerization and structural properties intermediate between those of temperate zone fish and terrestrial vertebrates. The presence of intracellular urea concentrations of approximately 400 mM in elasmobranchs (Yancey et al., 1982) may be a selective factor in establishing the structural and functional properties of elasmobranch proteins (Yancey & Somero, 1979; Yancey et al., 1982).

In conclusion, the differences found in the ΔH and ΔS of the G to F transformation among actins of differently adapted species suggest that evolutionary changes in muscle actins have occurred that effect a stabilization of the C_c at physiological temperatures. The interspecific differences in polymerization thermodynamics and structural stabilities are suggestive of two types of mechanism for adjusting assembly energetics: alterations in the types of weak bonds between subunits and variations in the energy costs of effecting conformational changes (G-actin to G*-actin) in the actin monomer.

Acknowledgments

We thank Drs. Richard Haedrich and Eugene Copeland for their assistance in obtaining the deep-sea fishes and Dr. Ted DeLaca for providing the Antarctic fishes.

References

Blikstad, I., Markey, F., Carlsson, L., Persson, T., & Lindberg, U. (1978) *Cell (Cambridge, Mass.) 15*, 935–945.

Brandts, J. F. (1969) in *Structure and Stability of Biological Macromolecules* (Timascheff, S. N., & Fasman, G. D., Eds.) pp 213–290, Marcel Dekker, New York.

Brenner, S. L., & Korn, E. D. (1981) *J. Biol. Chem. 256*, 8663–8670.

Carlsson, L., Nystrom, L.-E., Sundkvist, I., Markey, F., & Lindberg, U. (1977) *J. Mol. Biol. 115*, 465–483.

Chothia, C., & Janin, J. (1975) *Nature (London) 256*, 705–708.

Cooke, R. (1975) *Biochemistry 14*, 3250–3256.

Engelborghs, Y., Heremans, K. A. H., & DeMaeyer, L. C. M. (1976) *Nature (London) 259*, 686–689.

Fisher, H. F., Colen, A. H., & Medary, R. T. (1981) *Nature (London) 292*, 271–272.

Frank, H. S., & Evans, M. W. (1945) *J. Chem. Phys. 13*, 507–532.

Gordon, D. J., Yang, Y., & Korn, E. D. (1976) *J. Biol. Chem. 251*, 7474–7479.

Greaney, G. S., & Somero, G. N. (1979) *Biochemistry 18*, 5322–5332.

Harwell, O. D., Sweeney, M. L., & Kirkpatrick, F. H. (1980) *J. Biol. Chem. 255*, 1210–1220.

Higashi, S., & Oosawa, F. (1965) *J. Mol. Biol. 12*, 843–865.

Hitchcock, S. E., Carlsson, L., & Lindberg, U. (1976) *Cell (Cambridge, Mass.) 7*, 531–542.

Houk, T. W., Jr., & Ue, K. (1974) *Anal. Biochem. 62*, 66–74.

Ikkai, T., & Ooi, T. (1966) *Biochemistry 5*, 1551–1560.

Ikkai, T., Ooi, T., & Noguchi, H. (1966) *Science (Washington, D.C.) 152*, 1756–1757.

Josephs, R., & Harrington, W. F. (1968) *Biochemistry 7*, 2834–2847.

Junowicz, E., & Spencer, J. H. (1973) *Biochim. Biophys. Acta 312*, 72–84.

Kasai, M. (1969) *Biochim. Biophys. Acta 180*, 399–409.

Kasai, M., Asakura, S., & Oosawa, F. (1962) *Biochim. Biophys. Acta 57*, 13–21.

Kauzmann, W. (1959) *Adv. Protein Chem. 14*, 1–63.

Krug, R. R., Hunter, W. G., & Grieger, R. A. (1976) *Nature (London) 261*, 566–567.

Lauffer, M. A. (1975) *Mol. Biol., Biochem. Biophys. 20*, 264.

Lazarides, E., & Lindberg, U. (1974) *Proc. Natl. Acad. Sci. U.S.A. 71*, 4742–4746.

Lehrer, S. S., & Kerwar, G. (1972) *Biochemistry 11*, 1211–1217.

Lindberg, U. (1964) *Biochim. Biophys. Acta 82*, 237–248.

Lumry, R., & Biltonin, R. (1969) in *Structure and Stability of Biological Macromolecules* (Timasheff, S. N., & Fasman, G. D., Eds.) pp 65–212, Marcel Dekker, New York.

Lumry, R., & Rajender, J. (1970) *Biopolymers 9*, 1125–1227.

Mannherz, H. G., Leigh, J. B., Leberman, R., & Pfrang, H. (1975) *FEBS Lett. 60*, 34–38.

Norris, K. S. (1953) *Ecology 34*, 265–287.

Oosawa, F., & Kasai, M. (1971) *Biol. Macromol. 5*, 261–322.

Reisner, A. H., Nemes, P., & Bucholtz, C. (1975) *Anal. Biochem. 64*, 509–516.

Rich, S. A., & Estes, J. E. (1976) *J. Mol. Biol. 104*, 777–792.

Somero, G. N. (1982) in *Ecosystem Processes in the Deep Oceans* (Ernst, W. G., & Morin, J., Eds.) Prentice-Hall, New York (in press).

Spudich, J. A., & Watt, S. (1971) *J. Biol. Chem. 246*, 4866–4871.

Spudich, J. A., & Cooke, R. (1975) *J. Biol. Chem. 250*, 7485–7491.
Stevens, C. L., & Lauffer, M. A. (1965) *Biochemistry 4*, 31–37.
Strzelecka-Golaszewska, H., Prochniewicz, E., Nowak, E., Zymorzynski, S., & Drabikowski, W. (1980) *Eur. J. Biochem. 104*, 41–52.
Uyemura, D. G., Brown, S. S., & Spudich, J. A. (1978) *J. Biol. Chem. 253*, 9088–9096.
Vandekerckhove, J., & Weber, K. (1978) *Nature (London) 276*, 720–721.
Vandekerckhove, J., & Weber, K. (1979) *FEBS Lett. 102*, 219–222.
Weber, K., & Osborn, M. (1969) *J. Biol. Chem. 244*, 4406–4412.
Weisenberg, R. C. (1972) *Science (Washington, D.C.) 177*, 1104–1105.
Whitaker, J. R., & Granum, P. E. (1980) *Anal. Biochem. 109*, 156–159.
Wrigley, C. W. (1971) *Methods Enzymol. 22*, 559–564.
Yancey, P. H., & Somero, G. N. (1979) *Biochem. J. 183*, 317–323.
Yancey, P. H., Clark, M. E., Hand, S., Bowlus, R. D., & Somero, G. N. (1982) *Science (Washington, D.C.)* (in press).

Sulfhydryl Chemistry and Solubility Properties of Human Plasma Apolipoprotein B†

Alan D. Cardin, Kathleen R. Witt, Carole L. Barnhart, and Richard L. Jackson*

ABSTRACT: Apolipoprotein B (apoB) was isolated from human plasma low-density lipoproteins (LDL; d = 1.02–1.05 g/mL) by delipidation with ether–ethanol, followed by solubilization of the protein with sodium decyl sulfate. After the detergent was reduced to <0.1 μg of sodium decyl sulfate/mg of protein by dialysis, apoB was next precipitated with ethanol to remove residual lipids and then solubilized in 6 M guanidine hydrochloride (Gdn-HCl). Dialysis of apoB in 6 M Gdn-HCl against 10 mM tris(hydroxymethyl)aminomethane hydrochloride (Tris-HCl), pH 8.5, resulted in protein precipitation; however, dialysis against 6 M urea and then 10 mM Tris-HCl, pH 8.5, resulted in a water-soluble apoprotein. Water-soluble apoB gave a single precipitin line of complete identity with LDL when tested by immunodiffusion against anti-apoB. ApoB contains 13.9 ± 0.1 mol of half-cystine residue/250 000 g of polypeptide. Twelve of these residues form six intramolecular disulfide bonds in LDL while two SH groups remain free. Intermolecular disulfide bonds are formed during lipid extraction of LDL, yielding high molecular weight aggregates of apoB. The cross-linking reaction occurs by a sulfhydryl–disulfide exchange mechanism and is catalyzed by the two free SH groups originally present on each apoB molecule in LDL. Alkylation of the free SH groups with iodoacetamide blocks the exchange reaction. However, the addition of glutathione to carboxamidomethylated apoB promotes intermolecular disulfide exchange, yielding high molecular weight aggregates. The formation of intermolecular disulfide bonds occurs at the expense of intramolecular disulfide bonds and relieves secondary structural restraints. In addition, both intra- and intermolecular disulfide bonds impose modest restraints on the tertiary structure of apoB as determined by circular dichroism (CD) methods. Analysis of the far-UV CD region of apoB at various purification steps suggests that the conformation and state of association are the major factors contributing to the overall water solubility of apoB in the absence of denaturants and amphiphilic ligands.

The low-density lipoproteins (LDL)[1] of human plasma contain a high molecular weight apoprotein, apolipoprotein B (apoB), which functions in the transport of lipid to extrahepatic cells (Brown & Goldstein, 1979; Brown et al., 1978). This apoprotein has a molecular weight of 250 000 in concentrated Gdn-HCl as determined by ultracentrifugation (Steele & Reynolds, 1979b), although studies based on quantitative chemical analysis suggest the possibility of a lower unit molecular weight for apoB (Bradley et al., 1978). The structural characterization of apoB has been greatly compounded by its insolubility in aqueous buffers; detergents, denaturants (Gotto et al., 1973; Helenius & Simons, 1971; Shore & Shore, 1967; Day & Levy, 1968; Scanu et al., 1968; Pollard et al., 1969; Kane et al., 1970; 1980; Chen & Aladjem, 1978; Steele & Reynolds, 1979a; Lee, 1976), or other proteins (Shireman et al., 1977) are required for its solubilization. ApoB can also undergo extensive aggregation (Steele & Reynolds, 1979b; Socorro & Camejo, 1979), and it is highly susceptible to intact chain degradation by proteolytic

† From the Division of Lipoprotein Research, Departments of Pharmacology and Cell Biophysics, Biological Chemistry, and Medicine, University of Cincinnati College of Medicine, Cincinnati, Ohio 45267. *Received January 18, 1982; revised manuscript received April 29, 1982.* This work was supported by U.S. Public Health Service Grant HL-23019 and by General Clinical Research Center Grant RR-00068. A.D.C. is supported by National Institutes of Health Training Grant HL-07382.

* Address correspondence to this author at the Department of Pharmacology and Cell Biophysics, University of Cincinnati Medical Center, Cincinnati, OH 45267.

[1] Abbreviations: VLDL, very low density lipoproteins; LDL, low-density lipoproteins; HDL, high-density lipoproteins; apoB, a major protein constituent of chylomicrons, VLDL, and LDL; DPPC, dipalmitoylphosphatidylcholine; CD, circular dichroism; MCD, magnetic circular dichroism; PMSF, phenylmethanesulfonyl fluoride; EDTA, disodium salt of ethylenediaminetetraacetic acid; CAM-apoB, carboxamidomethylated apoB; RCAM-apoB, reduced and carboxamidomethylated apoB; DTNB, 5,5′-dithiobis(2-nitrobenzoic acid); GSH, reduced form of glutathione; BHT, butylated hydroxytoluene; CAM-LDL, carboxamidomethylated LDL; Gdn-HCl, guanidine hydrochloride; Tris-HCl, tris(hydroxymethyl)aminomethane hydrochloride.

0006-2960/82/0421-4503$01.25/0